

This copy is for your personal, non-commercial use only.

If you wish to distribute this article to others, you can order high-quality copies for your colleagues, clients, or customers by [clicking here](#).

Permission to republish or repurpose articles or portions of articles can be obtained by following the guidelines [here](#).

The following resources related to this article are available online at www.sciencemag.org (this information is current as of January 19, 2011):

Updated information and services, including high-resolution figures, can be found in the online version of this article at:

<http://www.sciencemag.org/content/329/5995/1068.full.html>

Supporting Online Material can be found at:

<http://www.sciencemag.org/content/suppl/2010/08/25/329.5995.1068.DC1.html>

A list of selected additional articles on the Science Web sites **related to this article** can be found at:

<http://www.sciencemag.org/content/329/5995/1068.full.html#related>

This article **cites 20 articles**, 4 of which can be accessed free:

<http://www.sciencemag.org/content/329/5995/1068.full.html#ref-list-1>

This article has been **cited by** 1 article(s) on the ISI Web of Science

This article has been **cited by** 3 articles hosted by HighWire Press; see:

<http://www.sciencemag.org/content/329/5995/1068.full.html#related-urls>

This article appears in the following **subject collections**:

Genetics

<http://www.sciencemag.org/cgi/collection/genetics>

Genomic Comparison of the Ants *Camponotus floridanus* and *Harpegnathos saltator*

Roberto Bonasio,^{1*} Guojie Zhang,^{2,3*} Chaoyang Ye,^{4*} Navdeep S. Mutti,^{5*} Xiaodong Fang,^{3*} Nan Qin,^{3*} Greg Donahue,⁴ Pengcheng Yang,³ Qiye Li,³ Cai Li,³ Pei Zhang,³ Zhiyong Huang,³ Shelley L. Berger,^{4†} Danny Reinberg,^{1,6†} Jun Wang,^{3,7†} Jürgen Liebig^{5†}

The organized societies of ants include short-lived worker castes displaying specialized behavior and morphology and long-lived queens dedicated to reproduction. We sequenced and compared the genomes of two socially divergent ant species: *Camponotus floridanus* and *Harpegnathos saltator*. Both genomes contained high amounts of CpG, despite the presence of DNA methylation, which in non-Hymenoptera correlates with CpG depletion. Comparison of gene expression in different castes identified up-regulation of telomerase and sirtuin deacetylases in longer-lived *H. saltator* reproductives, caste-specific expression of microRNAs and SMYD histone methyltransferases, and differential regulation of genes implicated in neuronal function and chemical communication. Our findings provide clues on the molecular differences between castes in these two ants and establish a new experimental model to study epigenetics in aging and behavior.

As eusocial insects, ants live in populous colonies in which up to millions of individuals delegate the reproductive role to one or few queens, while nonreproductive workers carry out all tasks required for colony maintenance (1). These mutually exclusive morphologies and behaviors arise from a single genome and are typically dictated not by genetic

differences, but by environmental factors (2). The first fertilized (diploid) eggs laid by a founder queen develop into workers, but as the colony enlarges, some diploid embryos take a different developmental path to become virgin queens, which leave the nest, mate, and establish new colonies. As colonies mature, queens transition from a broad behavioral repertoire that allows them to forage, excavate nests, and rear offspring, to one restricted to egg-laying and total dependence on workers. Queens also live up to 10 times longer than workers and 500 times longer than males (3).

We compared the genomes of the ants *Camponotus floridanus* and *Harpegnathos saltator*, because of contrasts in their behavioral flexibility, caste specialization, and social organization. *C. floridanus* lives in large organized colonies, in which only the queen lays fertilized eggs; when the queen dies, so does the colony (1). Non-reproductive individuals belong to two separate castes, major and minor workers, which exhibit differences in morphology and behavior established during development purely on environmental grounds. In contrast, the *H. saltator* social

system and division of labor are more basal: dimorphism between queens and workers is limited, and when the queen dies she is replaced by workers that become functional queens, called gamergates (4).

These two ant species differ in other respects as well. *C. floridanus* are scavengers, forage diurnally and nocturnally, and lay pheromone trails that mark paths to food sources. *H. saltator* workers prey on small arthropods in a solitary and diurnal fashion. *C. floridanus* exhibits high territoriality, strong nestmate recognition, and elaborate task specialization. In contrast, *H. saltator* displays low territoriality, loses nestmate recognition in the laboratory, and has only basic task specialization.

The Illumina Genome Analyzer platform was used to sequence genomic libraries for *C. floridanus* and *H. saltator*, obtaining more than 100-fold coverage. Draft genomic assemblies reached scaffold N50 size of ~600 kb (table S1), although for *C. floridanus* most genome-wide analyses reported here were conducted on an earlier version (v3), with scaffold N50 size of 444 kb (table S1). Assembly resulted in only small gaps and large N50 size, which assured us that most genomic features, particularly gene models, were predicted with reasonable accuracy. We verified the assemblies by sequencing 9 (*C. floridanus*) and 10 (*H. saltator*) randomly selected fosmid inserts (average size, 37 kb) (table S2). Additionally, we sequenced ~5000 expressed sequence tags from each ant and mapped them to the assembled scaffolds; more than 95% matched the assemblies (table S3).

The *C. floridanus* and *H. saltator* assemblies cover more than 90% of the genomes, which we estimate at 240 and 330 Mb in size, respectively (fig. S1 and table S4). The *H. saltator* assembly contains 45% G+C, similar to *Drosophila melanogaster* (42%), and *Nasonia vitripennis* (42%), whereas the *C. floridanus* genome is A+T rich, with a G+C frequency of 34%, similar to *Apis mellifera* (33%) (5) (table S4). Organisms that use DNA methylation for gene regulation typically display a depletion of CpG dinucleotides in their genome (table S5); however, CpG dinucleotides are overrepresented in both ant genomes

¹Department of Biochemistry, New York University School of Medicine, 522 First Avenue, New York, NY 10016, USA.

²Chinese Academy of Sciences–Max Planck Junior Research Group, State Key Laboratory of Genetic Resources and Evolution, Kunming Institute of Zoology, Chinese Academy of Sciences, Kunming, Yunnan 650223, China. ³Beijing Genomics Institute–Shenzhen, Shenzhen 518083, China. ⁴Department of Cell and Developmental Biology, University of Pennsylvania School of Medicine, Philadelphia, PA 19104, USA. ⁵School of Life Sciences, Arizona State University, Tempe, AZ 85287, USA. ⁶Howard Hughes Medical Institute, New York University Medical School, New York, NY 10016, USA. ⁷Department of Biology, University of Copenhagen, Copenhagen DK-2200, Denmark.

*These authors contributed equally to this work.

†To whom correspondence should be addressed. E-mail: berger@mail.med.upenn.edu (S.L.B.); danny.reinberg@nyumc.org (D.R.); wang@genomics.cn (J.W.); juergen.liebig@asu.edu (J.L.)

Fig. 1. Ant proteome. Phylogenetic tree based on maximum likelihood analyses of a concatenated alignment of single-copy proteins (left), and orthology relationships in multiple insects (right), using *Homo sapiens* as outgroup. The scale bar indicates 0.1 substitution per site. *T. castaneum*, *Tribolium castaneum*; *B. mori*, *Bombyx mori*; *A. gambiae*, *Anopheles gambiae*.

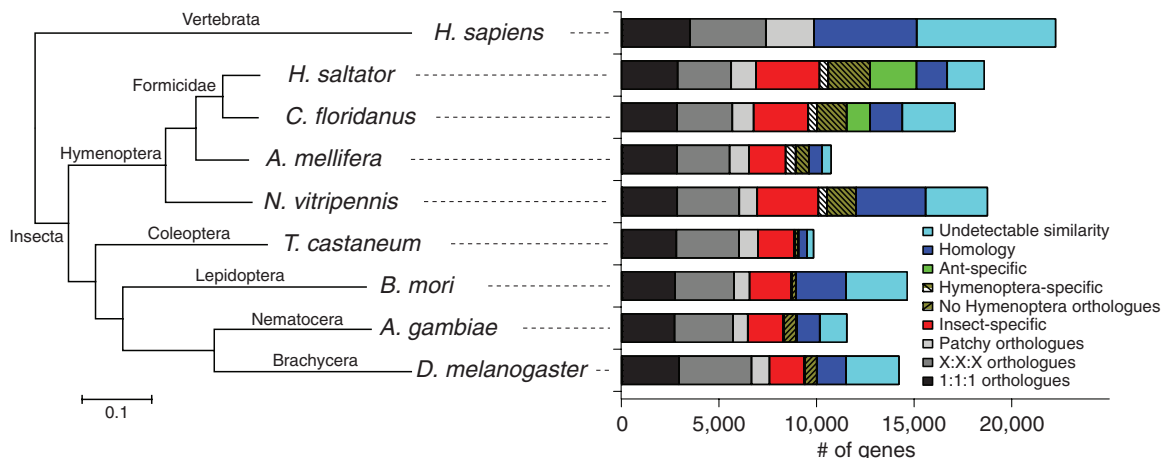


(table S4 and fig. S2), despite the presence of cytosine methylation. CpG dinucleotides are also overrepresented in *A. mellifera* (5) and in *N. vitripennis*; thus, this genomic feature may be specific to the Hymenoptera.

Repetitive elements constitute 15% of the assemblies in *C. floridanus* and 27% in *H. saltator* (table S4 and fig. S3), which is probably an underestimate, because genome regions that cannot be assembled are enriched in repeats. Both genomes contain copies of the *piggyBac* transposon [234 in total and 6 with intact open reading frames (ORFs) in *C. floridanus*, 976 in total and 23 with intact ORFs in *H. saltator*], which has been used for insect transgenesis (6, 7) and may also prove useful in ants.

Segmental duplications (SDs) account for 9.6% and 14.8% of the *C. floridanus* and *H. saltator* genomes, respectively (table S6). The 1810 (*C. floridanus*) and 2858 (*H. saltator*) gene models found in SDs are enriched in Gene Ontology (GO) terms associated with chemodetection, olfactory function, and protease/peptidase activity (table S7). *C. floridanus* SDs are also enriched for genes belonging to the cytochrome P450 family—perhaps as a result of detoxifying needs related to their generalist feeder life-style.

The predicted proteomes of *C. floridanus* and *H. saltator* share most protein families with *A. mellifera* and *N. vitripennis*, but also contain a large number of ant-specific (690) and species-specific families (3230 in *C. floridanus* and 2617 in *H. saltator*) without homologs in the other two Hymenoptera (fig. S4). When more insect ge-

nomes are included in the comparison, one-third of the ant protein-coding genes are conserved with vertebrates and two-thirds are conserved with insects, leaving 506 ant-specific protein families and 2000 to 3000 species-specific families (Fig. 1). Ant-specific genes were enriched not only in GO terms “olfactory receptor activity,” “sensory perception of smell,” “G protein-coupled receptor activity,” and “odorant binding,” but also in terms related to detoxification, including “monooxygenase activity” and “heme binding” (table S8).

We annotated 96 microRNA (miRNA) genes in *C. floridanus* and 159 in *H. saltator*. These accounted for most of the small RNA reads in adult specimens, with the exception of *H. saltator* gamergates, which showed a larger proportion of small RNAs mapping to unannotated regions of the genome (Fig. 2A and table S9). Gamergates also expressed the most diverse miRNA repertoire (table S10). The two *C. floridanus* worker castes displayed differential expression of miRNAs, with *cflo-mir-64* up-regulated in minor workers (Fig. 2B) and *cflo-mir-7* in major workers (fig. S5). This suggests that, in addition to being developmentally regulated (Fig. 2, C and D), some miRNAs might contribute to the differences among ant castes.

We examined the ant genomes and transcriptomes for signatures related to aging. Telomere shortening is a hallmark of cellular senescence in multicellular eukaryotes, and the enzyme telomerase (*TERT*), which counteracts telomere shortening, prolongs life span upon overexpression (8). *TERT* RNA levels were highest in eggs and

lower in adults in both *C. floridanus* and *H. saltator*, but they were up-regulated in *H. saltator* gamergates (Fig. 3A). This may be explained by the gamergates acquiring many physiological characteristics of queens, including longer life span (9). Aging has also been linked to the sirtuin lysine deacetylases SIRT1 and SIRT6, homologous to the *Saccharomyces cerevisiae* Sir2p implicated in replicative senescence (10). In *H. saltator* gamergates, both of these genes are expressed at higher levels compared to workers (Fig. 3B). These results suggest that the regulation of life span in gamergates may share common mechanisms with other organisms.

The caste system in ant societies in general, and the social flexibility of *H. saltator* in particular, allow us to study the role of epigenetics in behavior, aging, and development. Here, we use the term “epigenetics” as the ensemble of molecular pathways that select genomic regions (chromatin domains) for activation or repression, transmit these states through cell division, and stabilize them in differentiated cell types. These mechanisms include DNA methylation, histone posttranslational modifications, and trans-acting mechanisms involving noncoding RNAs (11).

Unlike in *Drosophila*, DNA methylation pathways in *A. mellifera* and *N. vitripennis* are similar to those of mammalian systems (5, 12). In the two ant species, we found single copies of cytosine methyltransferases *DNMT1* and *DNMT3B* genes and the noncatalytic *DNMT3L*, as well as four genes containing methyl-CpG binding domains (table S11). Consistent with these and previous observations (13), we detected the presence of 5-methylcytosine in the ants genomic DNA. *H. saltator*, which shows more ancestral characteristics, had less DNA methylation than its more derived relative, *C. floridanus* (Fig. 4A).

Histone acetyltransferases (HATs) and deacetylases (HDACs) add and remove acetyl groups on histone tails, regulate genes through chromatin structure (14), and are linked to the aging process (10). We identified 26 putative HATs in *C. floridanus* and 27 in *H. saltator*, with an expansion of GCNLT2 homologs (table S12). Humans have four classes of HDACs, comprising HDAC1–11 and the NAD⁺-dependent sirtuin family proteins (SIRT1–7). In contrast, only four HDACs and six sirtuins are found in *A. mellifera* (5). We identified five HDACs in *C. floridanus* and four in *H. saltator*, as well as six sirtuins in both ant species (table S11). Compared with mammals, these two ants and the honeybee lack SIRT3 (10).

Histone methylation is suspected to participate in epigenetic processes (11). We identified 27 proteins containing the conserved SET histone methyltransferase domain in *C. floridanus* and 22 in *H. saltator* (table S13). All major SET families are conserved in ants, including Polycomb/trithorax group, NSDs, SMYDs, and SETDs, and the arginine methyltransferase family. The SMYD family appears to have undergone multiple duplication events during the evolution of insects (fig. S6). We found five homologs in *C.*

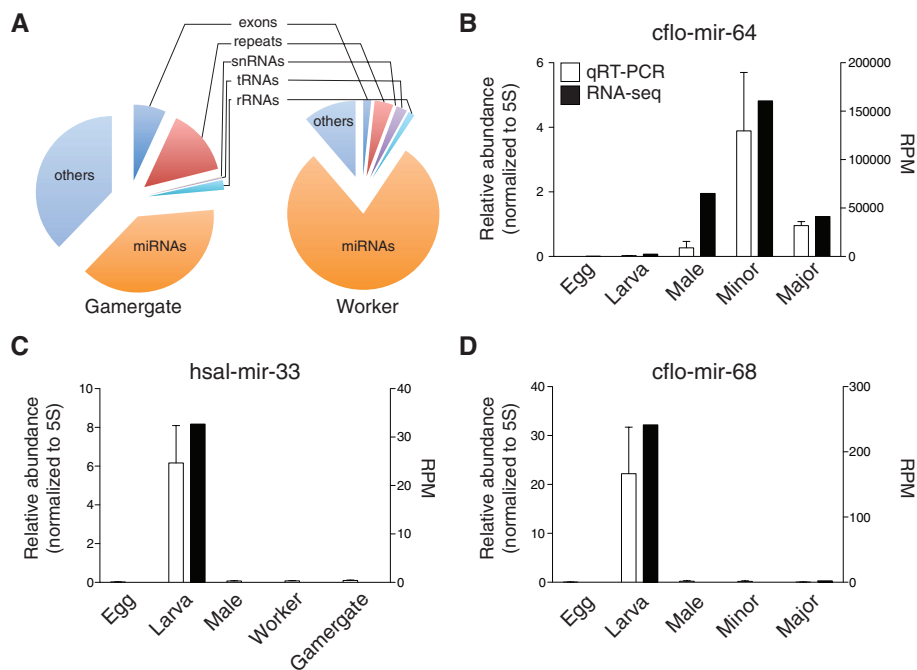


Fig. 2. Small RNA-seq and miRNA. **(A)** Classification of small RNA-seq reads from *H. saltator* gamergates (left) or workers (right). snRNAs, small nuclear RNAs; rRNAs, ribosomal RNAs. **(B to D)** Caste- and stage-specific expression of miRNAs in *C. floridanus* [(B) and (D)] and *H. saltator* (C). White bars represent quantitative reverse transcription–polymerase chain reaction (qRT-PCR) and indicate the mean \pm SEM, $n = 7$ biological replicates. Black bars are scaled on the right y axis and indicate reads per million (RPM).

floridanus and six in *H. saltator* of *SMYD4*, which is involved in muscle development and breast cancer (15, 16). *SMYD* family members

are differentially regulated among different ant castes and developmental stages (fig. S7); among them, a *SMYD3* homolog (Hsal_14941) is up-

regulated in gamergates (Fig. 4B), whereas a *SMYD4* homolog (Hsal_08142) is up-regulated in nonreproductive workers (Fig. 4C).

The elaborate social organization in ant colonies is attributed to a sophisticated communication system, made up of chemical signals that elicit behavioral responses via the nervous system (1). Many enriched GO terms associated with differentially expressed genes in *C. floridanus* (table S14) and *H. saltator* (table S15) castes are related to neuronal function and chemical communication. In *C. floridanus* major and minor workers, we detected differences in the expression levels of genes associated with GO terms including “postsynaptic membrane,” “ligand-gated channel activity,” “sensory perception of smell” (table S14), and “neurotransmitter binding” (Fig. 5A). This suggests that the different behaviors exhibited by distinct workers castes may in part be encoded in the brain at the transcriptional level.

Olfactory receptors (ORs) are G protein-coupled receptors (GPCRs) that function in behavioral responses and chemical communication in animals (17). We found 139 genes containing the *Drosophila* olfactory receptor domain (IPR004117) in *C. floridanus* and 105 in *H. saltator* (tables S16 and 17). Similar to the *A. mellifera* genome, the ant genomes contain fewer gustatory receptors and odorant binding proteins than *Drosophila* (tables S16 and 17). The number of identified ORs is much smaller than the number of glomeruli observed in the antennal lobe for both ant species (18, 19), apparently contradicting findings in other insects, which showed that most ORs are individually represented in the brain by a dedicated glomerulus (20). However, our homology-based approach might be insufficient to detect all ant-specific ORs.

In ants, cuticular hydrocarbons play a key role in nestmate recognition and regulation of reproduction (21). GO terms associated with the metabolism of hydrocarbons were enriched in ant-specific protein families (table S8) and in protein families expanded in ants (table S18 and fig. S8). *C. floridanus* and *H. saltator* have 19 and 14 genes, respectively, containing a beta-ketoacyl synthase domain (IPR014030), whereas *A. mellifera* has 3 and *D. melanogaster* has 4. Genes with putative roles in hydrocarbon metabolism show altered expression levels across castes and developmental stages (fig. S9). Compared to nonreproductive workers, *H. saltator* gamergates up-regulated several hydrocarbon metabolism genes, including homologs of a fatty acid synthase (*FASN*), an acetyl-coenzyme A desaturase (*SCD*), and an elongase of very long fatty acid (*ELOVL4*) (Fig. 5B). *H. saltator* gamergates advertise their reproductive status to nestmates via long cuticular hydrocarbons (22), and we found that expression of most genes with homology to human *ELOV* genes was up-regulated in gamergates (fig. S10). Because of the complexity of the metabolic pathways involved, we cannot conclude that transcriptional regulation of these genes is directly linked to communication; however, these observations suggest a molecular basis for

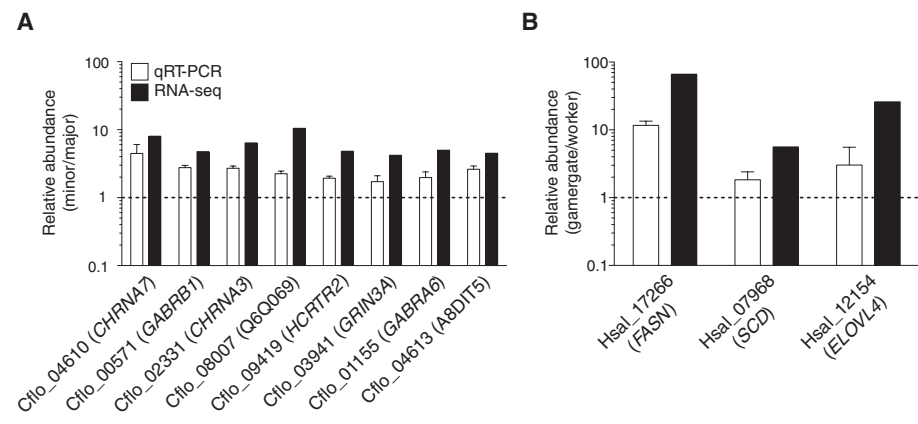
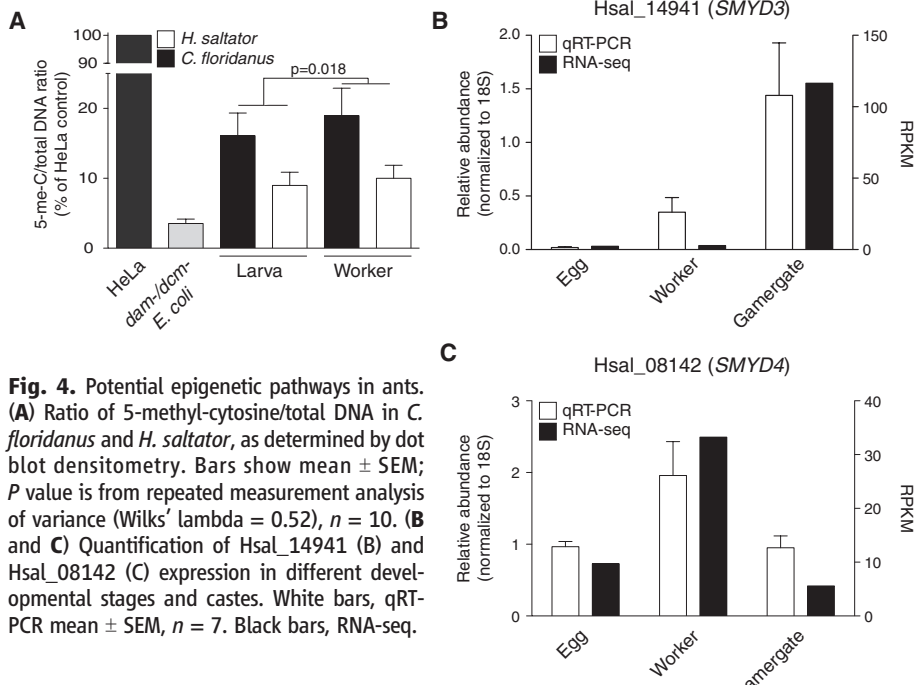
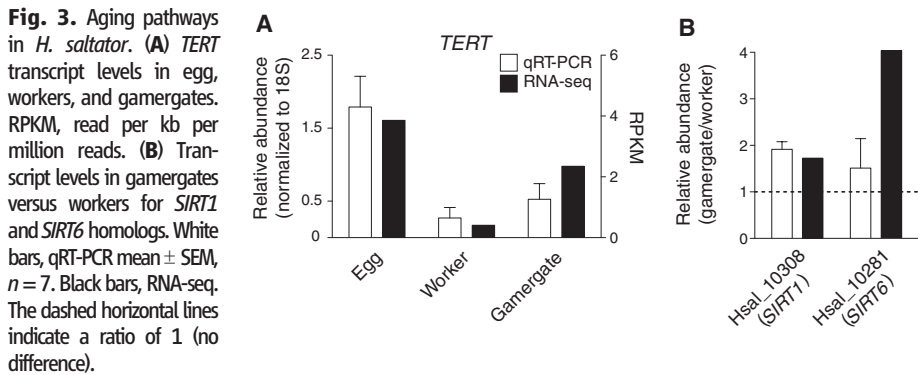


Fig. 5. Neurobiology and communication. (A) Quantification of 8 “GO:neurotransmitter binding” genes in head and thorax from major and minor workers in *C. floridanus*. White bars, qRT-PCR mean \pm SEM, $n = 9$. Black bars, RNA-seq. (B) Quantification of fatty acid biosynthesis genes in *H. saltator* gamergates compared to nonreproductive workers. White bars, qRT-PCR mean \pm SEM, $n = 7$. Black bars, RNA-seq.

the interplay between pheromone production, olfaction, and behavior in ants.

Our initial analysis of the genomes of two socially divergent ant species has captured major molecular features that make ants an attractive model for genomic and epigenetic studies. Ant species vary widely in the extent to which eusociality is implemented, ranging from small and less organized colonies to massive and complex societies (*1*). The diversity and flexibility of ants may provide experimental avenues to address long-standing hypotheses on the relationships among epigenetics, neurobiology, and behavior (*23*), as well as life-span regulation.

References and Notes

- Hölldobler, E. O. Wilson, *The Ants* (Harvard Univ. Press, Cambridge, MA, 1990).
- D. E. Wheeler, *Am. Nat.* **128**, 13 (1986).
- S. Jemielity, M. Chapuisat, J. Parker, L. Keller, *Age (Omaha)* **27**, 241 (2005).
- C. Peeters, J. Liebig, B. Hölldobler, *Insectes Soc.* **47**, 325 (2000).
- Honeybee Genome Sequencing Consortium, *Nature* **443**, 931 (2006).
- M. D. Lorenzen *et al.*, *Insect Mol. Biol.* **16**, 265 (2007).
- M. Sumitani, D. S. Yamamoto, K. Oishi, J. M. Lee, M. Hatakeyama, *Insect Biochem. Mol. Biol.* **33**, 449 (2003).
- E. Sahin, R. A. Depinho, *Nature* **464**, 520 (2010).
- A. Hartmann, J. Heinze, *Evolution* **57**, 2424 (2003).
- A. Vaquero, D. Reinberg, *Genes Dev.* **23**, 1849 (2009).
- C. D. Allis, T. Jenuwein, D. Reinberg, *Epigenetics*, M. Caparros, Ed. (Cold Spring Harbor Laboratory, Cold Spring Harbor, NY, ed. 1, 2007).
- J. H. Werren *et al.*, Nasonia Genome Working Group, *Science* **327**, 343 (2010).
- M. R. Kronforst, D. C. Gilley, J. E. Strassmann, D. C. Queller, *Curr. Biol.* **18**, R287 (2008).
- Z. Wang *et al.*, *Cell* **138**, 1019 (2009).
- E. C. Thompson, A. A. Travers, L. Randau, *PLoS ONE* **3**, e3008 (2008).
- L. Hu, Y. T. Zhu, C. Qi, Y. J. Zhu, *Cancer Res.* **69**, 4067 (2009).
- J. G. Hildebrand, G. M. Shepherd, *Annu. Rev. Neurosci.* **20**, 595 (1997).
- C. Zube, C. J. Kleinedam, S. Kirschner, J. Neef, W. Rössler, *J. Comp. Neurol.* **506**, 425 (2008).
- S. C. Hoyer, J. Liebig, W. Rössler, *Arthropod Struct. Dev.* **34**, 429 (2005).
- E. Fishilevich, L. B. Vosshall, *Curr. Biol.* **15**, 1548 (2005).
- G. J. Blomquist, A. G. Bagnères, *Insect Hydrocarbons: Biology, Biochemistry, and Chemical Ecology* (Cambridge Univ. Press, Cambridge, 2010).
- J. Liebig, C. Peeters, N. J. Oldham, C. Marktädter, B. Hölldobler, *Proc. Natl. Acad. Sci. U.S.A.* **97**, 4124 (2000).
- C. Dulac, *Nature* **465**, 728 (2010).
- We thank T. Bloss for ant colony maintenance, B. Kopenhaver for technical help, A. Alekseyenko and J. Wang for bioinformatic support, W. Wang for advice on evolutionary analysis, and P. Voigt and D. Simola for careful reading of the manuscript. R.B. is a fellow of the Helen Hay Whitney Foundation. This work was funded by Howard Hughes Medical Institute Collaborative Innovation Award #2009005 to S.L.B., D.R., and J.L. Raw sequencing data have been deposited in the National Center for Biotechnology Information as SRA020747 (*C. floridanus* genome), SRA020748 (*H. saltator* genome), and GSE22680 (RNA-seq). Assemblies and annotations have been deposited at DNA Data Bank of Japan–European Molecular Biology Laboratory–GenBank under the accession AEAB00000000 and AEAC00000000. The versions described in this paper are the first deposited versions: AEAB01000000 and AEAC01000000.

Supporting Online Material

www.sciencemag.org/cgi/content/full/329/5995/1068/DC1
Materials and Methods
SOM Text
Figs. S1 to S24
Tables S1 to S40
References

18 May 2010; accepted 20 July 2010
10.1126/science.1192428

Crystal Structure of Human Adenovirus at 3.5 Å Resolution

Vijay S. Reddy,^{1*} S. Kundhavi Natchiar,¹ Phoebe L. Stewart,² Glen R. Nemerow^{1*}

Rational development of adenovirus vectors for therapeutic gene transfer is hampered by the lack of accurate structural information. Here, we report the x-ray structure at 3.5 angstrom resolution of the 150-megadalton adenovirus capsid containing nearly 1 million amino acids. We describe interactions between the major capsid protein (hexon) and several accessory molecules that stabilize the capsid. The virus structure also reveals an altered association between the penton base and the trimeric fiber protein, perhaps reflecting an early event in cell entry. The high-resolution structure provides a substantial advance toward understanding the assembly and cell entry mechanisms of a large double-stranded DNA virus and provides new opportunities for improving adenovirus-mediated gene transfer.

Human adenoviruses (HAdV) are non-enveloped double-stranded DNA (dsDNA) viruses that are associated with acute infections (*1–3*). Although these infections are generally self-limiting, the reemergence of certain HAdV types has also been linked to potentially fatal respiratory infections in both civilian and military populations (*4*). Severe disseminated diseases also occur in patients receiving bone marrow–derived stem cells (*5, 6*). In addition to their disease associations, replication-defective or conditionally replicating HAdVs continue to be evaluated in ~25% of approved phase I to III clinical trials for vaccine and therapeutic gene

transfer (*7, 8*). However, the lack of accurate details of the virus structure limits the reengineering of HAdV vectors and prevents a better understanding of the virus life cycle. High-resolution HAdV structure determination presents a challenge because of the large size (910 Å average diameter, 150 megadalton) and complexity (pseudo-*T* = 25) of the virus. The crystal structures of the major HAdV capsid proteins, the fiber (*9*), penton base (PB) (*10*), and hexon (*11*), have been solved. The hexon and penton base crystal structures were subsequently used to derive pseudo-atomic models of the HAdV capsid at moderately high resolution (7 to 10 Å) (*12–14*) by cryoelectron microscopy (cryoEM). CryoEM structural analyses provided considerable insight into HAdV organization; however, they did not furnish detailed information on the interactions between the major and accessory (cement) proteins (IIIa, VI, VIII, and IX).

We report here the crystal structure of a recombinant HAdV-5 vector, designated Ad35F,

that is equipped with a short and flexible fiber protein derived from HAdV-35 (*15*). Details of the crystallization (*16*), diffraction data statistics (table S1), and structure determination of Ad35F at near-atomic resolution (3.5 Å) are described in (*17*).

The architecture of the HAdV capsid is shown in Fig. 1, A and B. The hexon is the most abundant protein in the capsid, with 720 subunits arranged as 240 trimers on a pseudo-*T* = 25 icosahedral lattice. Five PB monomer subunits occupy each of the icosahedral vertices and are associated with the trimeric fiber protein. Each of the 20 facets of the capsid contains 12 hexon trimers and a penton at each vertex. The icosahedral asymmetric unit consists of four hexon trimers and one PB monomer. As previously described, each hexon monomer contains two eight-stranded jelly-roll domains, V1 and V2 (*11*), whereas the PB subunit contains a single jelly-roll domain (*10*). Three sets of V1 and V2 domains give the hexon trimer a pseudo-hexagonal shape at the base, which in turn gives rise to a pseudo-*T* = 25 architecture for the HAdV capsid. Large insertions between the strands of the hexon jelly-roll domains form triangular towers on top of the hexagonal base. Representative electron density for a hexon subunit [amino acids (aa) 579 to 582] is shown in fig. S1. Some of the hypervariable region loops (aa 186 to 193 and 250 to 258) that were disordered in the isolated hexon structure are visible in the HAdV capsid crystal structure (fig. S1) because they are involved in multiple, symmetry-related interhexon contacts (figs. S2 and S3). The tertiary structures of the 12 structurally independent hexon subunits are nearly identical, having a root mean square deviation of ~1 Å upon superposition with a few differences found mainly at the amino and carboxy termini.

¹The Scripps Research Institute, 10550 North Torrey Pines Road, La Jolla, CA 92037, USA. ²Vanderbilt University Medical Center, 2215 Garland Avenue, 710 Light Hall, Nashville, TN 37232, USA.

*To whom correspondence should be addressed. E-mail: gnemerow@scripps.edu (G.R.N.); reddyy@scripps.edu (V.S.R.)